Title

An ultrasensitive test for profiling circulating tumor DNA using integrated comprehensive droplet digital detection

Journal

Lab on a Chip, 19(6)

ISSN

1473-0197

Authors

Ou, Chen-Yin

Vu, Tam

Grunwald, Jonathan T

et al.

Publication Date

2019-03-13

DOI

10.1039/c8lc01399c

Peer reviewed

HHS Public Access

Author manuscript

Lab Chip. Author manuscript; available in PMC 2020 March 13.

Published in final edited form as:

Lab Chip. 2019 March 13; 19(6): 993–1005. doi:10.1039/c8lc01399c.

An Ultrasensitive Test for Profiling Circulating Tumor DNA using Integrated Comprehensive Droplet Digital Detection

Ou Chen-Yin[a,#], **Tam Vu**[b,f,#], **Jonathan T. Grunwald**[a], **Michael Toledano**[b], **Jan Zimak**[b], **Melody Toosky**[a], **Byron Shen**[a], **Jason A. Zell**[d,h], **Enrico Gratton**[f,i], **Tim Abram**[a,*], and **Weian Zhao**[b,c,d,e,f,g,h,*]

[a]Velox Biosystems, 5 Mason, Suite 160, Irvine, CA 92618, USA;

[b]Sue and Bill Gross Stem Cell Research Center, University of California, Irvine, Irvine, CA 92697, USA;

[c]Department of Pharmaceutical Sciences, University of California, Irvine, Irvine, CA 92697, USA;

[d]Chao Family Comprehensive Cancer Center, University of California, Irvine, Irvine, CA 92697, USA;

[e]Edwards Life Sciences Center for Advanced Cardiovascular Technology, University of California, Irvine, Irvine, CA 92697, USA;

[f]Department of Biomedical Engineering, University of California, Irvine, Irvine, CA 92697, USA;

[g]Department of Biological Chemistry, University of California, Irvine, Irvine, CA 92697, USA;

[h]Division of Hematology/Oncology, University of California Irvine Medical Center, Orange, USA;

[i]Laboratory for Fluorescence Dynamics, Department of Biomedical Engineering, University of California, Irvine, USA;

Abstract

Current cancer detection systems lack the required sensitivity to reliably detect minimal residual disease (MRD) and recurrence at the earliest stages when treatment would be most effective. To address this issue, we present a novel liquid biopsy approach that utilizes an Integrated Comprehensive Droplet Digital Detection (IC3D) digital PCR system which combines microfluidic droplet partitioning, fluorescent multiplex PCR chemistry, and our rapid 3D, large-volume droplet counting technology. The IC3D ddPCR assay can detect cancer-specific, ultra-rare genomic targets due to large sample input and high degree of partitioning. We first demonstrate

*Corresponding authors: Dr. Weian Zhao, Sue & Bill Gross Hall CIRM Institute, 845 Health Sciences Road, Suite 3027, Irvine, CA, 92697, USA; Office Phone: 949-824-9744; weianz@uci.edu, Dr. Tim Abram, Velox Biosystems, 5 Mason, Suite 160, Irvine, CA, 92618, USA; tabram@veloxbio.com.

Author contributions

Formal analysis: T.A., T.V.; Methodology: T.A., W.Z., C.O., T.V.; Writing - original draft: C.O., T.V., T.A., W.Z.; Investigation: C.O., T.V., M.T., J.Z., M.T.; Data curation: C.O., T.V., J.G., T.A.; Conceptualization: W.Z., C.O., T.V., B.S., T.A.; Resources: W.Z., J.Z., E.G.

#Co-first authors

Conflicts of interest

Weian Zhao is the founder of Velox Biosystems Inc that develops in vitro diagnostics.

Electronic Supplementary Information (ESI) available: [details of any supplementary information available should be included here]. See DOI: 10.1039/x0xx00000x

our droplet digital PCR assay can robustly detect common cancer mutants including KRAS G12D spiked in wild-type genomic background or isolated from patient samples with 100% specificity. We then demonstrate that the IC3D ddPCR system can detect oncogenic KRAS G12D mutant alleles against a background of wild-type genomes at a sensitivity of 0.00125 – 0.005% with a false positive rate of 0% which is 50 to 1,000× more sensitive than existing commercial liquid biopsy ddPCR and qPCR platforms, respectively. In addition, our technology can uniquely enable detection of circulating tumor cells using their genetic markers without a pre-enrichment step, and analysis of total tumor DNA isolated from blood samples, which will increase clinical sensitivity and specificity, and minimize inter-assay variability. Therefore, our technology holds the potential to provide clinicians with a powerful decision-making tool to monitor and treat MRD with unprecedented sensitivity for earlier stage intervention.

Graphical Abstract

We present an ultra-sensitive, novel liquid biopsy approach which can uniquely enable detection of CTCs using genetic markers without pre-enrichment.

Introduction

At some point during their lifetimes, approximately 38.4% of men and women will be diagnosed with cancer.[1] Colorectal cancer (CRC), in particular, is the third most commonly diagnosed cancer, and the third most common cause of cancer-related deaths in the United States. In 2018, it is estimated that 140,000 people were diagnosed with CRC, and 50,000 people succumbed to the disease.[2] Despite major advances in treatment (i.e., surgery, radiation therapy, chemotherapy, biologic/immune therapy) and resultant improved outcomes over time, colorectal cancer survivors with potentially curable (non-metastatic) disease still face a 10 – 50% risk of relapse. Relapse carries an extremely high mortality risk, as most relapses are not curable by current methods, except in cases of oligometastatic disease, where surgical resection of limited areas of tumor burden may result in cure. As such, monitoring for minimal residual disease (MRD) in CRC survivors has become a major investigational focus, as advances in MRD detection are expected to lead to early intervention and improved outcomes for this deadly disease. National Comprehensive Cancer Center Network (NCCN) Guideline-based surveillance monitoring with clinical exams, serial serum carcinoembryonic antigen testing, annual imaging assessments, and regular colonoscopic evaluations, however, lack the required sensitivity and/or specificity to reliably detect MRD at the earliest stages when treatment would be most effective.[3]

Mounting evidence has recently demonstrated that “liquid biopsy” blood tests for cancer biomarkers, i.e., circulating tumor cells (CTC), circulating cell-free tumor DNA (ctDNA), and exosomes, can serve as a non-invasive, cost effective and viable alternative for cancer detection, surveillance monitoring of MRD, and drug response evaluation.[4,5] The use of liquid biopsy can 1) avoid invasive and repeated tumor sampling involved in conventional tissue biopsy or toxic radiation exposure involved in conventional imaging modalities, and 2) better recapitulate real-time genetic profiles in the tumor as a whole, which can be missed in traditional biopsies due to intra-tumor heterogeneity. Several liquid biopsy tests have been FDA-approved, including the CellSearch System for CTC and the PCR-based Cobas®

EGFR Mutation Test v2 for non-small cell lung cancer.[6] Many other methodologies including various CTC isolation and enrichment methods, digital PCR (dPCR) and Next-Generation Sequencing (NGS) for cell-free DNA (cfDNA) are being developed and validated in the pipeline by both academia and industry worldwide, as surveyed in recent reviews.[7,8] Early clinical validation of these liquid biopsy approaches has led to promising results as it can provide actionable information to potentially improve clinical outcome. For instance, Diehl et al.[9] demonstrated that PCR measurements of cfDNA aberrations (e.g., APC, TP53 and KRAS) in the plasma could be used to reliably detect residual disease and monitor tumor dynamics in CRC patients who were undergoing surgery or chemotherapy. Furthermore, Tie et al.[10] demonstrated that sequencing of cfDNA after stage II CRC resection could identify patients at high risk for recurrence to help stratify treatment decisions.

Despite these early promises, detecting and monitoring cancer via liquid biopsy assays have yet to transform routine practice in clinical oncology. A major current limitation is the poor sensitivity of existing platforms to efficiently and effectively detect low-abundance circulating cancer biomarkers especially for early-stage cancers, MRD, and recurrence.[11] For instance, the abundance of cfDNA and CTCs in patients with early stage disease is known to be significantly lower (10-fold) than those in patients with more advanced stages. Various reports have also demonstrated that CTCs can exist in low numbers in blood (<1–100 CTC/ml).[8,12] As a result, it was estimated that only 30–40% of stage I and II cancers could be detected using current methods. For cell surface protein capture approaches, the use of single or multiple surface protein markers (e.g., EpCAM) in the CellSearch system and other methods are inadequate to capture and detect all CTCs. Alternatively, detection of CTCs using direct genetic analyses has been largely impractical due to the vast background of genomic, wild-type (WT) DNA contributed from white blood cells; therefore, an enrichment step is inevitably needed prior to their analysis. Indeed, the current assays for tumor DNA detection including qPCR (e.g., PNA clamp-PCR and ARMS), digital PCR (dPCR)(e.g., BEAMing and Bio-Rad droplet digital PCR (ddPCR)), and NGS have been confirmed to possess a sensitivity of only 0.01%−1%.[13] The challenges with detection of CTCs have resulted in a shift in the field to the detection of cfDNA in plasma. However, for cfDNAs that exist in low total quantities (typically 10s ng/ml) and are surrounded by excess WT DNA in plasma, these assays have been notably inadequate to detect these rare targets in early stage cancer patients. Furthermore, recent studies have suggested that CTCs, cfDNAs, and other circulating cancer markers including exosomes are distinct entities; therefore, each of them alone may not be adequate to reveal complete profiles of cancer.[14–17] Additionally, different isolation and sample processing kits and protocols for each of these cancer marker subtypes have created large variabilities and inconsistences between different settings, which represents a major roadblock to fully realize liquid biopsy's potential to cancer management in the clinic.

We reason the sensitivity and robustness of cancer liquid biopsy tests that use circulating tumor DNA as markers can be greatly improved using a dPCR platform that can accommodate 1) much larger DNA sample input, 2) greater numbers of partitions, and 3) total DNA isolated from blood samples regardless of their origins in a single assay. dPCR formats permit absolute quantitation of target DNA with improved sensitivity and precision

compared to qPCR assays. The compartmentalization of target DNA in droplets or microwells significantly increases the effective target concentration following PCR while reducing interference from background (WT genomic DNA), to permit absolute, digital ("1" or "0") quantification without the need for calibration curves. Despite these advances, existing dPCR assays still lack the required sensitivity for rare target DNA detection in the context of early stages of cancer, MRD, and recurrence due to their limited input sample content and number of partitions. For instance, Bio-Rad's QX-200 ddPCR assay can only handle 20 μL sample volumes (approximately 20,000 droplets) at a time with typically 0–66 ng of intact DNA input per single reaction.[18–20] Each run can thus accommodate only a small fraction of the total DNA isolated from several mls of blood samples, an amount typically required in order to detect rare targets effectively without subsampling issues.[21–23]

We recently developed a platform technology called Integrated Comprehensive Droplet Digital Detection (IC3D) that can selectively detect biomarkers from large volumes of biological samples such as bacteria in blood or circulating miRNA in plasma at single-cell or single-molecule sensitivity with a limit of detection (LOD) of single-digit number of targets per ml of measurement volume.[24,25] Our system integrates target-specific fluorescent chemistry, droplet microfluidics, and a high throughput 3D particle counting system. Unlike conventional particle-counting systems (e.g., flow cytometry and 1D on-chip droplet counting in the Bio-Rad ddPCR system) that have low throughput and, therefore, can only accommodate a small sample volume or require multiple runs and much longer time to analyze greater sample volume, the IC3D system can robustly detect fluorescent particles from ml volumes (tens of millions of droplets) at single-particle sensitivity within several minutes by collecting droplets in a cuvette and analyzing them in bulk using a high throughout 3D particle counter (Figure 1). In this study, we evaluated IC3D as a novel ddPCR platform for ctDNA detection in cancer liquid biopsy. We demonstrated that the unique capabilities of rapid and large volume (ml) analysis of IC3D allow us to accommodate a significantly higher amount of DNA (20 μg/ml) and greater numbers of partitions (18 million reactions/ml), compared to commercial assays such as Bio-Rad ddPCR and qPCR. As a proof of concept, we demonstrated that our system can achieve a sensitivity improvement of at least 50- to 1,000-fold compared to Bio-Rad ddPCR and qPCR, respectively. In addition, we demonstrated cancer cells spiked in blood (modelling CTCs) can be directly analyzed with IC3D ddPCR using their genetic markers without the need for pre-enrichment. Therefore, unlike previous studies that have to profile cfDNA, CTCs, or other ctDNA carriers separately, the IC3D system provides additional ability to analyze these markers together in a single assay from the same blood draw to greatly increase clinical sensitivity and specificity and reduce inter-assay variability.

Materials and methods

Materials

Phosphate-buffered saline (PBS, 10×) without Ca^{2+} and Mg^{2+} salts and bovine serum albumin (BSA) were purchased from Sigma-Aldrich (Saint Louis, MO). RPMI 1640 and DMEM with L-glutamine, were purchased from VWR (Radnor, PA). Fetal bovine serum (FBS), and penicillin/streptomycin (PS) were purchased from Invitrogen (Carlsbad, CA). All

primers and probes used for this study were purchased from LGC Biosearch Technologies and Integrated DNA Technologies (IDT) and their sequences are listed in Supplementary Table 1. Synthetic and HPLC-purified KRAS G12D and BRAF V600E mutants were synthesized as double-stranded gBlocks® gene fragments and verified by IDT to guarantee the accuracy of the sequences (details regarding the synthetic gene fragments are listed in Supplementary Table 2). PerfeCTa qPCR ToughMix was purchased form Quanta BioSciences. Nuclease-free water, Rox reference dye (50×) and Countess cell counting chamber slides (for microscopic imaging of the droplets) were purchased from Thermo-Fisher Scientific (Waltham, MA). SU-8 2075 negative photoresist and developer were purchased from Microchem (Newton, MA). Silicon 4 in. wafers were purchased from University Wafer (South Boston, MA). Photomasks were purchased from CAD/Art Services (Bandon, OR). Sylgard 184 polydimethylsiloxane (PDMS) and curing agent were purchased from Ellsworth Adhesives (Concord, CA). PFPE-based surfactant was prepared by Velox Biosystems with our proprietary formulation. HFE-7500 fluorocarbon oil was purchased from 3M (St. Paul, MN).

Primers, probes, and gBlocks preparation

Primers and probes from LGC Biosearch Technologies and IDT were centrifuged at 8,000 rpm for 1 minute and reconstituted to a final concentration of 100 μM in TE buffer (10 mM Tris, 0.1 mM EDTA, pH 8.0). Following IDT recommended procedures, KRAS c.35G>A (G12D) and BRAF c.1799T>A (V600E) gBlock® gene fragments were reconstituted to a final concentration of 10–20 ng/μl in TE buffer. A NanoDrop 2000 Spectrophotometer (Life Technologies) was used to assess the purity, quality, and concentrations of gene fragments. Primers, probes, and gene fragments were stored in DNA LoBind tubes at −20 °C prior to experiments.

Cell-lines and DNA sample preparation

The human colon adenocarcinoma cell line, LS174T (CL-188), and human T-cell lymphoblast cell line, Jurkat E6–1 (TIB-152), were obtained from the American Type Culture Collection (ATCC). LS174T cells were cultured in DMEM media while Jurkat cells were cultured in RPMI 1640 media, both supplemented with L-glutamine, 10% FBS, and 1% PS. All cells were cultured at 37 °C with 5% atmospheric CO_2 in a humidified incubator. Prior to ddPCR or blood spiking experiments, cells were cultured in flasks until sub-confluence, trypsinized (if adherent), resuspended in PBS, and then subjected to either genomic DNA (gDNA) extraction protocols or to whole blood titration experiments. For gDNA extraction, QIAamp Blood DNA miniprep kit (Qiagen) was used according to manufacturer's instructions, and a NanoDrop 2000 Spectrophotometer (Life Technologies) was used to assess the purity and quality of these purified gDNA samples. Only DNA samples with absorbance ratios of $A_{260/280}$ and $A_{260/230}$ greater than 1.8 were used for this study.

Healthy donor samples

De-identified and healthy donor blood samples used in this study were obtained with informed consent from donors and approval from the Institutional Review Board (IRB 2012–9023) via the Blood Donor Program at the UCI Institute for Clinical and Translational

Science (ICTS). Samples were collected in lavender top (K2EDTA) vacutainer tubes using venipuncture under sterile conditions and processed within several hours for downstream experiments.

CRC patient samples

A clinical pilot study was completed to validate the ability of our system to detect and quantify SNP cancer mutations in patient plasma. IRB-exempted and de-identified plasma samples from patients diagnosed with CRC (n = 7, average age = 59, stages I to III) were purchased from BioIVT (Westbury, NY). These samples were pre-determined to be positive for KRAS G12D by genetic sequencing by the vendor. As negative controls, non-screened plasma samples from healthy patients were obtained from the aforementioned ICTS donor program. In brief, cfDNA was extracted from 1 ml of patient plasma samples using a QIAamp Circulating Nucleic Acid kit (Qiagen, Cat#: 55114), following manufacturer's protocols. Purified cfDNA was eluted with Qiagen AE buffer and stored at −20 °C in DNA LoBind tubes prior to ddPCR assays. For ddPCR assays, purified cfDNA samples were mixed with a PCR master mix containing 0.5 μM primers and 0.25 μM probe specific against KRAS G12D (Supplementary Table 1) before droplet encapsulation using a flow-focusing microfluidic device. Droplet PCR conditions for this set of experiments were 95 °C for 3 min (1 cycle), 95 °C for 20 s and 60 °C for 20 s (40 cycles), and 4 °C (hold) using a C1000 Touch Thermal Cycler (Bio-Rad). After thermocycling, droplets were imaged on a fluorescent microscope as described below and median droplet fluorescence intensity was measured. Droplets were defined to be positive for KRAS G12D if they had a minimum signal-to-noise ratio of 3.0 compared to background non-fluorescent droplets.

IC3D digital droplet system

The IC3D platform technology has been utilized for a number of different applications including the detection of bacterial species-specific targets in blood using DNAzyme sensors and detection of circulating miRNA in plasma using EXPAR probes.[24,25] Without modifying the scanning instrumentation, we have adapted this platform into a droplet digital PCR assay by employing and optimizing several technical parameters including droplet size, DNA loading content, and the use of propynyl-dC (pdC) and propynyl-dU (pdU) modified dual-labelled PCR probes in order to detect ultra-rare circulating tumor DNA targets with high sensitivity and SNP-specific selectivity in this present study.

Microfluidic chip design and fabrication

We employed a custom microfluidic chip design with the architectures and operating mechanism described in Figure 2. The fabrication for this four-nozzle droplet generation platform was based on a modified version of an established soft lithography procedure.[24] Microchannel architectures were designed using AutoCAD (Autodesk, San Rafael, CA, USA) and sent to CAD/ART services (Bandon, OR, USA) who provided high-resolution photomasks. SU-8 master molds were produced with the recommended protocol from Micro-Chem. After wafer fabrication, PDMS was mixed in a 1:10 ratio of curing agent to elastomer and subsequently degassed and poured onto the SU-8-on-Si wafer master. PDMS was cured in an oven for 4 hours at 95 °C. Once cured, PDMS layers were peeled off and punched with a 1 mm diameter biopsy punch (Kay Industries Co., Tokyo, Japan) to create

inlets and outlets. To bond PDMS to glass, both surfaces were treated with oxygen plasma in a PDC-32G Harrick Plasma Cleaner (Harrick Plasma, Ithaca, NY) for 30 s and bound together. Finally, the droplet generation devices were post-baked in a convective oven at 95 °C for at least 24 hours.

Droplet Generation

Samples were emulsified with the use of 3M™ Novec™ HFE-7500 Engineered Fluid (fluorinated oil) containing 2% PFPE surfactant. For the disperse phase, aqueous solutions containing PCR reagents and DNA sample were loaded into syringes on top of 200 μl of HFE-7500 fluorocarbon oil without surfactant to displace sample volume and ensure full encapsulation of the aqueous layer. A second syringe was loaded with fluorinated oil with 2% PFPE surfactant to serve as the continuous phase. Both syringes were mounted onto PHD Ultra™ syringe pumps (Harvard Apparatus) and connected to the respective aqueous and oil inlets on the microfluidic chip. Droplet generation was monitored with optical microscopes (Celestron® LCD Digital Microscope) to ensure consistent droplet production. Droplets were prepared for each sample using separate devices to avoid contamination and were collected in sterile collection tubes.

Microscope evaluation of droplet PCR assay performance

Microscope images of a 2D monolayer of droplets were recorded to evaluate droplet generation uniformity, droplet thermal stability, and PCR efficiency. Approximately 10 μl of droplets were dispensed onto a disposable hemocytometer (Invitrogen™ Countess Cell Counting Chamber Slides) prior to analysis. Quantitative measurements for each of these evaluations included average droplet diameter and %CV before and after thermocycling (using brightfield imaging at 10× magnification) and signal-to-noise ratios computed from median fluorescence signal intensity of droplets from a positive control sample (using fluorescence imaging (FITC) at 10× magnification).

Sample preparation for droplet partitioning experiment

To demonstrate the effects of rainfall on assay performance as higher concentrations of wild-type gDNA are loaded, 300 μl of PCR reaction mixture containing (PerfeCTa qPCR ToughMix reagent (1×), NP-40, forward and reverse primers (1 μM each), mutant probe (0.25 μM)), and 225,000 copies of synthetic KRAS G12D mutant were mixed with 0.1, 0.5, 1, 2.5, 5 or 10 μg of gDNA isolated from Jurkat cells. Additionally, a blank sample (which does not contain wild-type Jurkat gDNA and KRAS G12D mutant) was also prepared as a non-template control. Fluorescent signal suppression (“rainfall”) was assessed via quantitative intensity measurements of 2-dimensional droplet microscopy images (described above).

Sample preparation for multiplex droplet digital PCR study

To demonstrate the capacity of multiplex droplet digital PCR to detect mutant alleles (MT) in the presence of wild-type genome backgrounds (WT) using 90 μm droplets, 100 μl of PCR reaction mixture (PerfeCTa qPCR ToughMix reagent (1×), NP-40, forward and reverse primers (1 μM each), wild-type probe (0.25 μM), mutant probe (0.25 μM)), containing

75,000 copies of synthetic targets (or 0 as negative control) were mixed with 250 ng of Jurkat gDNA (equivalent to 75,757 haploid genome copies) to reach an mutant allele frequency of ~50% (or 0% for negative control). For calculating gene copy number in gDNA, haploid copy number dilutions were calculated based on the molecular weight of one normal haploid female genome equalling 3.3 pg.[26]

Sample preparation for synthetic KRAS G12D study

For our test trial to assess the analytical sensitivity of our IC3D platform using 90 μm droplets, 850 μl of PCR reaction mixture (PerfeCTa qPCR ToughMix reagent (1×), NP-40, forward and reverse primers (1 μM each), mutant probe (0.25 μM)) containing different amounts of synthetic KRAS G12D targets (0, 68, 680, 3,400, 6,800, 34,000, 637,500 copies) were mixed with 2.125 μg of Jurkat gDNA (equivalent to 643,939 haploid genome copies) to reach mutant allele frequencies of 0, 0.01, 0.1, 0.5, 1, 5, and 50%, respectively.

Sample preparation for LS174T spiked blood experiment

To demonstrate the potential of our IC3D platform to detect CTCs in whole blood without pre-enrichment, we used the human colorectal adenocarcinoma model cell line, LS174T, to assess the analytical sensitivity of our assay. We spiked varying numbers of LS174T cells into 1 ml whole blood sample aliquots obtained from a healthy donor. Serial dilutions of LS174T prepared at 400k, 100k, 25k, 6.4k, 1.6k, 400, and 100 cells were spiked into each respective blood sample to establish a titration series that spans a broad dynamic range of sensitivity (Supplementary Table 3). To determine the wild-type leukocyte background of each sample, a set of three 1 ml blood samples from the same donor were lysed with an ACK lysis buffer kit (Thermo-Fisher). Red blood cells were fractionated and removed during the process while white blood cells were fully retained to allow precise and accurate leukocyte quantification on a hemocytometer. In short, 1 ml of EDTA-treated whole blood was diluted with ACK lysis buffer at a ratio of 1:10 and allowed to incubate at RT for 5 minutes for each replicate. The remaining leukocytes were centrifuged at 300 × g for 7 min at RT, washed with 4 °C cold PBS, centrifuged at 300 × g for 7 min at 4 °, and resuspended with 4 ° cold PBS. Following ACK lysis, leukocytes were mixed with trypan-blue and loaded into a Hausser Scientific 3100 hemocytometer (Thermo-Fisher). White blood cells were counted and averaged from 4 quadrants for each replicate and were determined to have an expected background concentration of 3.95×10^6 cells per ml. A QIAamp Blood DNA miniprep kit (Qiagen) was then used, according to manufacturer's instructions, to purify and isolate all gDNA from the LS174T-spiked whole blood samples. This kit contains the proteolytic agent, proteinase K, which lyses all cells in the blood samples and allows us to perform downstream PCR-based molecular detection without CTC loss. Purified gDNA samples were eluted with Qiagen AE buffer and stored at −20 °C in DNA LoBind tubes prior to experiments. Lastly, these samples were analyzed on a NanoDrop and determined to have absorbance ratios of $A_{260/280}$ and $A_{260/230}$ greater than 1.8. For IC3D experiments, each PCR condition utilized 6 μg of gDNA as template and had a final reaction volume of 300 μl. The PCR reactions contained PerfeCTa qPCR ToughMix reagent (1×), NP-40, forward and reverse primers (1 μM each), and mutant probe (0.5 μM). Due to the high concentration of background gDNA, samples were encapsulated in smaller 50 μm droplets in order to increase the fraction of binary droplets.

Droplet PCR

Prior to thermocycling, droplet samples were transferred to thin-walled PCR tubes, each containing 30 μL Novec™ 7500 oil with surfactant and 70 μL of droplets. For droplet PCR, the following PCR protocol was used: (1) 3 min at 95 °C (initial denaturation), (2) 20 sec at 95 °C (denaturation), (3) 60 sec at 58.1 °C, (4) Repeat Steps 2 & 3 for 40 cycles, and (5) an infinite 12 °C hold. Following thermocycling, samples were assessed via fluorescence microscopy (described above) and 3D fluorescent scanning (described below).

Droplet detection using 3D particle counter

The droplet scanning instrument used in this study consisted of a bench-top, horizontal-geometry confocal microscope. In this embodiment, a visible-wavelength excitation laser beam (λ = 469 nm with ~2.2 mW typical output power) was focused by an under-filled low numerical aperture 20× objective (MV-20×, Newport) inside a cylindrical cuvette (Abbott) containing the droplet sample. Slow (5 mm/s) vertical translation and fast (200 rpm) rotation of the cuvette transported the target fluorescent droplets across the Gaussian-shaped excitation volume. The emitted fluorescence signal was collected by the same objective, transmitted through a dichroic filter and collimated onto the sensitive area of a photomultiplier tube (H9305–04 PMT, Hamamatsu) for the time-trace acquisition.

Droplet samples for IC3D scanning were manually transferred from the individual PCR tubes of each sample into thoroughly cleaned, borosilicate glass cuvettes containing 1.5 ml of 3M™ Novec™ 7500 Engineered Fluid (fluorinated oil) with 2% surfactant and scanned for 2 minutes. Raw fluorescent time trace data collected from the droplet scanning instrument was analyzed using SimFCS (Laboratory for Fluorescence Dynamics, Irvine, CA, USA: www.lfd.uci.edu). To achieve high specificity while counting the number of detection events, the fluorescence time trace data was fit to a pre-determined Gaussian profile of fixed standard deviation and amplitude. Hits were only counted if the chi-square value of the shape-fit was statistically significant ($X^2 < 0.003$) and the peak amplitude was between a user-defined minimum and maximum threshold. Parameters were determined based on the highest concentrated sample in each of the following experiments to correctly identify hits with consistent widths and amplitudes and applied to remaining data (synthetic KRAS G12D study: SDV = 24, minimum amplitude threshold = 510 mV, maximum amplitude threshold = 3,000 mV, chi-square threshold = 0.003, LS174T cell-spiking study: SDV = 16, minimum amplitude threshold = 200 mV, maximum amplitude threshold = 5,000 mV, chi-square threshold = 0.01). (An SDV of 24 corresponds to a Gaussian peak of width equal to 145 data points, which at a sampling frequency of 64kHz is approximately 2.26 milliseconds). Though the shape-fitting algorithm utilized in the IC3D system can accurately differentiate positive, fluorescent droplets from other non-specific fluctuations in the recorded fluorescence signal, it does not exclude the possibility of false positives due to rare PCR false positive amplification.

qPCR for KRAS G12D mutant detection

Per 20 μl reaction volume, different amount of synthetic KRAS G12D targets (0, 16, 80, 160, 800, 1,700, 15,000 copies) and 50 ng of Jurkat gDNA were added to a PCR reaction mixture that included the following components: PerfeCTa PCR ToughMix reagent (1×),

NP-40, forward and reverse primers (1 μM each), mutant probe (0.25 μM), wild-type probe (0.25 μM) and 1× Rox. Each sample condition was run in quadruplicate (20 μl in each well) with 7900 HT Fast Real-Time PCR system (Applied Biosystems) using the same PCR thermal cycling condition as droplet PCR.

Assessing analytical sensitivity of Bio-Rad ddPCR QX-200 platform with LS174T spiked whole blood samples

To compare the performance of IC3D with the leading commercial ddPCR platform, we utilized the Bio-Rad QX-200 Digital PCR system (Bio–Rad Laboratories, Hercules, CA, USA) to assess the analytical sensitivity of this commercial ddPCR system in detecting CTCs in whole blood without pre-enrichment, using samples of LS174T spiked in whole blood. In brief, ddPCR reaction master mixes were made containing 10 μl of 2× ddPCR Supermix, 1 μl of 20× Human mutant KRAS p.G12D (c.35G>A) ddPCR FAM probe (dHsaCP2500596), 1 μl of 20× Human KRAS Wild-Type for p.G12D (c.35G>A) ddPCR HEX probe (dHsaCP2000002), 7 μl of nuclease-free water, and 1 μl of purified gDNA for each reaction. LS174T spiked whole blood samples were prepared in duplicates and at a concentration of 66 ng/μl based on manufacturer's recommendations for loading intact genomes. Furthermore, according to Bio-Rad's calculations and estimates of 1 haploid genome weighing 3.3 pg, 66 ng of DNA should contain 20,000 haploid genome equivalents (or gene copies if homozygous).[21,26] Each reaction mixture was then loaded into DG8 cartridges along with droplet generation oil to partition the samples using the QX-200 Droplet Generator. Thermal cycling conditions for this set of experiments were 95 °C for 10 min (1 cycle), 94 °C for 30 s and 55 °C for 1 min (40 cycles), 98 °C for 10 min (1 cycle) and 4 °C (hold). The QX-200 Droplet Reader was then used to assess droplets as positive or negative based on fluorescence amplitude and a set threshold. Data analysis was performed as recommended using the QuantaSoft Software version 1.7.4 and their Rare Mutation Best Practices Guidelines. A threshold of 2,500 was used for both mutant and WT channels to determine the fractional abundance of KRAS G12D for each LS174T spiked whole blood sample.

Validating KRAS G12D mutant allele frequency of LS174T with Bio-Rad QX-200 ddPCR

Upon contacting ATCC, we discovered that there has been no previous validation study conducted by the vendor to determine the mutant allele frequency (AF) of KRASG12D for the clonal cell line, LS174T. Based on existing independent reports and to our best knowledge, LS174T has been confirmed to express KRAS G12D but at variable frequencies depending on lab settings.[27–29] This prompted us to use the Bio-Rad QX-200 Digital PCR system (Bio–Rad Laboratories, Hercules, CA, USA) in order to accurately and precisely determine the percent mutant zygosity of our cell source. In brief, ddPCR reaction master mixes were made containing 10 μl of 2× ddPCR Supermix, 1 μl of 20× Human mutant KRAS p.G12D (c.35G>A) ddPCR FAM probe (dHsaCP2500596), 1 μl of 20× Human KRAS Wild-Type for p.G12D (c.35G>A) ddPCR HEX probe (dHsaCP2000002), 7 μl of nuclease-free water, and 1 μl of cell line gDNA for each reaction. LS174T or Jurkat (negative control) gDNA was prepared at a concentration of 12 ng/μl and added to PCR reaction mixtures in duplicates. As previously mentioned, with 1 haploid genome weighing 3.3 pg, 12 ng of DNA was expected to contain 3,636 haploid genome equivalents (or gene

copies if homozygous). The same droplet generation, PCR, and scanning conditions used on the Bio-Rad QX-200 platform described earlier were used for this set of experiments. For mutant zygosity confirmation, data analysis was performed as recommended by the manufacturer using the QuantaSoft Software version 1.7.4. Threshold was determined by comparing ddPCR results between Jurkat, LS174T, and a no template control (nuclease-free water).

Results and discussion

High-throughput droplet generation

The ability of the IC3D system to efficiently analyze large sample volumes is enabled by the combination of high-throughput droplet generation and rapid, three-dimensional scanning. While other design strategies have been utilized to demonstrate ultrahigh-throughput droplet generation,[30,31] the flow-focusing 4-nozzle droplet generator used in this study was chosen due to its ability to robustly generate precise droplets that maintain stability during thermocycling and its simple, single-layer fabrication and assembly (Figure 2.A). In order to improve device robustness by lowering the risk of nozzle clogging, a series of micro-posts with variable spacing were integrated into the aqueous and oil inlets to serve as an in-line filter (Figure 2.B). By altering the channel geometry at the nozzle region, devices were designed to produce droplets of various diameters. In this study, devices were fabricated to produce droplets with average diameters of 50 and 90 μm (Figure 2.C).

Flow rates for the aqueous and oil streams to produce stable 90 μm droplets were 50 μl/min and 75 μl/min, respectively and 15 μl/min and 80 μl/min, respectively for the production of stable 50 μm droplets. These flow rates correspond to droplet generation times of 66 min and 20 min for a 1 ml aqueous sample for 50 μm and 90 μm droplets, respectively. Droplet stability was assessed before and after 40 cycles of thermocycling by measuring droplet diameters in a 2-dimensional monolayer on a hemocytometer. Over a range of background gDNA content from 0 – 20 μg/ml, average diameters for the 50 μm before and after thermocycling were 50.11 μm (%CV = 3.73%) and 49.98 μm (%CV = 4.31%), respectively, while the 90 μm droplets averaged 91.56 μm (%CV = 3.60) before thermocycling and 91.62 μm (%CV = 3.28%) after thermocycling (Figure 2) (data from 20 unique fields of view with approximately 900–1,000 droplets per field for 50 μm droplets and 200–300 droplets per field for 90 μm droplets).

Droplet PCR assay

Somatic point mutations within tumoral DNA are highly specific biomarkers that can distinguish cancer cells from normal cells. These biomarkers have been shown to be applicable for cancer diagnosis, prognosis, selection of rational combination therapies, and monitoring of patients, but have yet to become routine assays employed in clinical oncology due to the unmet need for a more highly sensitive strategy that can discriminate tumor-specific mutations in a large excess of non-mutated DNA from normal cells. Nevertheless, the sensitivity of traditional approaches to SNP detection (techniques such as Sanger sequencing or TaqMan PCR) possess only a sensitivity of 1–10%,[32,33] thereby suffering from false negatives and limited reproducibility. A combination of conventional target-

specific TaqMan PCR and a droplet microfluidic system allows the partitioning of bulk PCR solution into a massive number of picoliter droplets in which each partition contains one or no target molecules. Partitioning of target mutant DNA away from highly homologous wild-type DNA permits absolute digital quantification of mutant targets with single-molecule sensitivity, reduces interference from background DNA, and, therefore greatly increases sensitivity over conventional approaches.

We first demonstrated the capacity of our system for multiplexed droplet digital PCR detection of different targets by detecting mutant alleles in the presence of wild-type genomic backgrounds (Figure 3). Primers and probes used for different SNP mutation detection (KRAS G12D and BRAF V600E, genetic markers among the most prevalent for CRCs and many other types of cancer) were designed and optimized to have the same annealing temperature for droplet digital PCR. Gene fragments carrying KRAS G12D or BRAF V600E were synthesized and sequence-verified by IDT, whereas background genomic DNAs harbouring wild-type KRAS and BRAF alleles were isolated and purified from Jurkat cells. In a 100 μl PCR volume, 250 ng of Jurkat gDNA was mixed with 75,000 mutant copies to reach approximately an equal molar ratio of wild-type to mutant copies. Using the droplet generation approach described previously, mutant copies as well as background DNA were compartmentalized in 90 μm droplets together with FAM probe specific for mutant targets and CAL560 probes specific for corresponding wild-type targets. Droplets were then thermocycled and the fluorescence signal of droplets was measured. The amplification of mutant DNA resulted in a green-fluorescent droplet while the amplification of wild-type DNA resulted in a red-fluorescent droplet. As shown in Figure 3, in the wild-type only control, only red-fluorescent droplets but not green-fluorescent droplets were observed. For samples containing both wild-type and mutant genes, the fluorescent droplets were either red (due to amplification of a wild-type gene), green (due to amplification of a mutant gene) or yellow (due to amplification of both a mutant and wild-type gene). This result suggests that we could specifically discriminate mutant alleles from wild-type alleles via a droplet digital PCR assay. While multiplex detection and analysis is possible with the IC3D system, the following studies demonstrate IC3D performance on SNP detection, using single-color mutation detection assays targeting KRAS G12D, one of the key and most prevalent cancer mutations associated in many different cancers for the remaining experiments.[34]

Analysis of KRAS G12D CRC patient samples

Furthermore, a pilot study using KRAS G12D mutant-positive (pre-determined by sequencing) CRC patient plasma samples (n=7) and healthy donor samples (n=5) demonstrated that our droplet PCR assay targeting KRAS G12D can accurately identify these cancer cases with 100% clinical sensitivity and specificity (Figure 4).

Demonstration of partitioning effect on assay sensitivity

Unlike commercially available dPCR systems, the IC3D technology can uniquely analyze large sample volumes, resulting in two key advantages: (1) the ability to load more volume (or DNA content) from a clinical sample per assay, and (2) the ability to achieve a higher degree of sample partitioning. To demonstrate the relationship between detection sensitivity

and the degree of sample partitioning, an experiment was performed using increasing amounts of genomic wild-type gDNA and measuring the total fraction of droplets that reached peak signal amplification. The increasing concentration of wild-type gDNA simulates the effect of generating fewer partitions for the same sample. Theoretical calculations for estimating the percent of "rainfall" (defined as the number of intermediate-intensity droplets divided by the total number of positive droplets) were based on partitioning statistics for a Poisson distribution as described in Milbury et al[35]. This theory estimates the probability of k targets in one droplet given an average "loading" of λ targets per droplet (λ_w = WT loading, λ_m = MT loading) as:

$$P(k;\lambda) = \frac{\lambda^k e^{-\lambda}}{k!}$$

Therefore, the rainfall fraction can be determined as the number of droplets containing both MT and WT copies divided by the total number of droplets containing MT copies, or N_{Dual}/N_{MT}:

$$\text{Rainfall fraction} = \frac{\left(1 - e^{-\lambda_w}\right) \cdot \left(1 - e^{-\lambda_m}\right)}{\left(1 - e^{-\lambda_m}\right)}$$

In theory, for digital PCR to be truly digital, a sample must be partitioned into only empty droplets and single-copy droplets (i.e. 0's and 1's, respectively) to achieve single-copy amplification. As seen in Figure 5, as the amount of WT gDNA background increases (and consequently the fraction of truly binary droplets decreases), the fraction of droplets at maximal PCR amplification decreases accordingly. This phenomenon, commonly referred to as "rainfall", exists when the binary partitioning condition is not met. In these scenarios, absolute quantification can result in inaccurate measurements. Additionally, as in the case of SNP detection where wild-type and mutant sequences are amplified with the same primer sequence, incomplete partitioning can yield droplets containing both mutant and wild-type copies which results in compromised detectable signal.

With its ability to accommodate very large sample volumes, the IC3D system can efficiently generate and analyze significantly more partitions than competing dPCR systems. Though different strategies exist for increasing the throughput of droplet detection in the context of ddPCR assays including large 2-dimensional arrays[36] and optofluidic devices,[37,38] the simplicity of the 3-dimensional droplet analysis technique presented here allows IC3D to scale easily to accommodate large sample volumes while maintaining exceptional sensitivity. In applications that require high concentrations of gDNA to be analyzed, the ability to interrogate significantly more partitions results in a higher fraction of truly binary droplets, which has the potential to greatly improve assay sensitivity.

IC3D ddPCR detection of synthetic KRAS G12D mutant in Jurkat gDNA

Plasma cell-free DNA (cfDNA) as a liquid biopsy assay has been shown to be a valuable surrogate specimen for detecting tumor-specific aberrations. However, detection of tumor-derived cfDNA has proven to be challenging in clinics, because tumor derived cfDNA often represents a small fraction (<1%) of total cfDNA.[32] We aimed to explore the clinical utility of detecting cfDNA isolated from plasma using IC3D. As a proof of concept, various copies of synthetic KRAS G12D mutant fragments were spiked into Jurkat gDNA (serving as the background of normal DNA), resulting in a wide range of mutant allele frequencies from 0.01% to 5%. In order to analyze these samples on the IC3D system, they were first encapsulated into 90 μm droplets (ensuring a high fraction of truly binary droplets), thermocycled to amplify the fluorescence signal from droplets containing the KRAS G12D target, and transferred to a cuvette for rapid 3-dimensional fluorescent scanning. Following scanning, the fluorescent time trace data was fit to a pre-determined shape fitting algorithm corresponding to the signal from true positive droplets and events were enumerated (Figure 6). As WT-containing droplets exhibit a dimly fluorescent signal in between the intensity of empty droplets and MT-containing droplets, stringent shape fitting algorithm parameters were selected to successfully differentiate positive droplets containing mutant targets (Figure 6c) from other non-specific fluctuations in the recorded fluorescence signal (Figure 6b).

We demonstrated that the full range of allele frequencies from 0.01% to 5% can be consistently detected with the IC3D system across three independent replicates (Figure 6). Furthermore, the aggregate response of all 3 replicates demonstrated a strong linear relationship between the sample concentration (0.01% - 5% AF) and the number of IC3D hits (adjusted $R^2 = 0.9723$). With a false positive rate of 0%, the IC3D system was able to detect all 3 replicates of the 0.01% AF sample. This experiment effectively demonstrated clinical feasibility of using IC3D for detecting cfDNA isolated from plasma.

For comparison, a conventional real-time PCR assay was performed for detection of synthetic KRAS G12D mutant allele frequencies of 0% (negative control), 0.1%, 0.5%, 1%, 5%, 10% and 50% in the presence of the same amount of background WT Jurkat gDNA (50 ng/20 μl). The KRAS G12D and WT targets were amplified with common primers, but differentiated by separate fluorescence-labelled BHQplus probes. The FAM-labelled probe targeted the KRAS G12D allele, while the CAL Fluor Orange560-labeled probe (VIC alternative probe) targeted the WT allele. In four replications per real-time PCR reaction, VIC fluorescence was detected in all samples with C_T (cycle threshold) values ranging between 25.1 – 25.7, indicating that a consistent level of WT background was present in all tested conditions. With regard to mutant detection, no FAM fluorescence was observed for the negative samples, but successful detection was observed in samples with 50% and 10% mutant allele frequencies (Supplementary Figure 2). However, no FAM fluorescence was detected for samples with 1%, 0.5%, and 0.1% mutant allele frequencies. For the 5% allele frequency sample, weak fluorescence was detected in two replications only, whereas no fluorescence was detected in the other two replications (Supplementary Figure 2). Hence, stable amplification was only observed for 10% mutant allele frequency samples or higher, indicating the lowest limit of detection by conventional real-time PCR for KRAS G12D detection with these study conditions is between 5% and 10% mutant allele frequency. By

comparison, the IC3D system demonstrated a 500-fold increase in sensitivity by detecting an allele frequency of 0.01% in an equivalent assay.

IC3D ddPCR detection of spiked LS174T cells in whole blood

We next evaluated the potential of IC3D ddPCR in analyzing total DNA isolated from blood specimens. Because the amount of cfDNA is negligible compared to DNA isolated from white blood cells, for simplicity, our model used healthy donor blood samples spiked with cancer cells in this set of experiments. Therefore, this study further allowed us to evaluate whether IC3D ddPCR can directly detect CTCs using genetic markers without a pre-enrichment step, which was largely impossible before due to the interference of WT gDNA background.

In this experiment, cancer cells harboring the KRAS G12D mutation were spiked into aliquots of unprocessed, whole blood. To accommodate this large genomic background, we utilized smaller droplets with an average diameter of 50 μm (compared to 90 μm in previous experiments) to achieve efficient partitioning of samples with a high background of gDNA (approx. 20μg/ml), resulting in the detection of between 100 – 400 cancer cells per ml of whole blood in this study (Figure 7) (false positive rate = 0%). By loading significantly more gDNA than demonstrated in the previous synthetic KRAS G12D detection study, an equivalent allele frequency between 0.00125% - 0.005% was detected in this experiment. Furthermore, increasing number of cells corresponded with an increase in the number of detected IC3D hit events and agreed well with results from the synthetic KRAS G12D detection study.

Comparison to Bio-Rad ddPCR

In order to determine the detection limit of the leading commercial ddPCR system using the same approach for KRAS G12D genetic detection of CTCs, a similar experiment was performed with samples from the same cell spiking dilution from above using the Bio-Rad QX-200 ddPCR system. Like many other conventional particle counting systems, droplets in the Bio-Rad ddPCR system are counted on a 1D, flow-based, on-chip system that operates at ~100s of particles/s with a relatively small number of parallel reactions (20 μL sample volume or 20,000 droplets).[21,39,40] Based on published guidelines for the Bio-Rad system, the maximum number of intact genomic DNA copies per 20 μl reaction volume is approximately 20,000 copies (or 66 ng per 20 μl reaction volume), above which the PCR reaction is inhibited.[21,41] We have found that the sensitivity of the Bio-Rad system is approximately 0.08 to 0.33% (i.e., 16 to 66 targets in 20,000 copies of genomic DNA) (Figure 7.c), which agrees with published studies from multiple groups concerning the detection of KRAS G12D.[42–45]

Data Analysis and Statistics

In order to assess the analytical performance of the IC3D and Bio-Rad ddPCR systems in terms of quantitation limit, we employed a simple definition of the analytical cutoff as the lowest measured concentration where the lower relative error bar does not cross the average false positive rate. Similar to the analytical cutoff used in the Bio-Rad's Rare Mutation Best Practice Guidelines, this metric establishes a straight-forward way of empirically

determining the limit of detection of each assay based on actual tested mutant positive and negative controls without contingency on theoretical extrapolation. For both systems, we defined the false positive rate as the average number of positive detection events (i.e. droplets) for negative control samples that contain an equivalent amount of WT but without the addition of LS174T cells.

Since the Bio-Rad's QuantaSoft software analysis tool allows for user-defined thresholding to define the acceptance criteria for positive events, we set a conservative threshold at 2,500, validated by the strong agreement of higher mutant fraction samples with expected mutant fractions (Supplementary Figure 1) [MF = 0.33 – 4.76%, confidence level > 96.9%]. Applying this same threshold to wells containing the wild type only negative control samples resulted in a false positive rate equivalent to a mutant fraction of approximately 0.07%, which agrees well with reported false positive rates exceeding 0.02% for KRAS G12D.[42–45] Due to this high false positive rate, the limit of detection for detecting CTCs spiked in whole blood on the Bio-Rad ddPCR system is 6,400 cells/ml (approximately 0.08% in allele frequency). Conversely, the high specificity of the IC3D detection and analysis platform facilitated by a robust shape-fitting algorithm resulted in a false positive rate of 0%, indicating a limit of detection of less than 400 cells/ml (approximately 0.005% in allele frequency). As a result, 2/3 replicates of 100 cells/ml (0.00125% allele frequency) and 3/3 replicates of 400 cells/ml (0.005% allele frequency) were in a detectable range above the negative control line. This suggests that our IC3D system can be used as a powerful tool to detect ctDNA from total DNA isolated from blood specimens with an allele frequency sensitivity at least 50-fold higher than the Bio-Rad ddPCR system per run. For additional context, the performance and throughput of the IC3D system as demonstrated in this study are compared to two commercial ddPCR systems in Supplementary Table 6. Therefore, we emphasize that droplet counting throughput is a critical performance metric which IC3D outperforms existing digital PCR systems.

Conclusions

We demonstrated that the IC 3D platform can greatly improve the sensitivity of ctDNA tests (i.e. at least 50 to 1,000× more sensitive than current dPCR and qPCR assays, respectively) due to larger sample input, and greater numbers of partitions. The IC3D platform uniquely enables analysis of total tumor DNA isolated from blood samples regardless of their origins (i.e. cfDNA, CTC DNA, or exosomal DNA), which will increase clinical sensitivity and specificity, and minimize biases of individual biomarkers and inter-assay variability due to pre-analytical preparations of individual markers. In fact, this is one of the first demonstrations that CTCs can be directly detected and profiled using their genetic markers without a pre-enrichment step, therefore eliminating the technical issues related to the efficiency of CTC purification and enrichment.[46,47] We expect our assay sensitivity can be further improved through genomic DNA digestion (more input sample loading), smaller droplets (more partitioning, as demonstrated by Pekin et al, 2011[26]) and the use of competitive probes such as PNA and XNA (higher SNR). We acknowledge that the Bio-Rad ddPCR and other systems can analyse large amount of DNA to achieve similar sensitivity if they run many parallel assays for a single sample (e.g. Bio-Rad ddPCR's 96 well-plate format), however, such implementation will incur significantly increased assay time and

cost. For instance, the Bio-Rad ddPCR system would need to run ~50 reactions (half of a 96 well-plate) to analyze 1 ml of blood in 2 hours, which would only require a single run using the IC 3D system in several minutes.

The inability of current technologies to sufficiently identify target ctDNA from a vast excess of wild-type counterparts especially in early-stage (Stages 0, I and II) cancers has limited the use of liquid biopsy for early detection and screening, prognosis, and treatment stratification. With this unprecedented high sensitivity, our IC3D assay has the potential to change how we detect, treat, and monitor cancer patients at an early stage when interventions are most effective. We are currently evaluating the prognostic implications of this IC3D ctDNA assay for MRD and recurrence detection in samples from early stage patients with CRC in an ongoing clinical study. In this study, we will have primary tumors genetically profiled and then run a targeted pre-defined tumor genetic panel using IC3D to guide personalized cancer monitoring and treatment. We emphasize that the IC3D technology intends to offer new capabilities (i.e., unprecedented high sensitivity) and to complement, rather than replace, existing technologies including NGS that can analyze broader genetic profiles. Finally, IC3D ddPCR assays can be applied to other areas where large sample input is required for rare target detection including HIV reservoir analysis, prenatal screening, and study of transplanted cells *ex vivo* in cell therapy.

Supplementary Material

Refer to Web version on PubMed Central for supplementary material.

Acknowledgements

This study is supported by NIH/NIAID (1 R01 AI117061), UCI Applied Innovation's Proof of Product (POP) Grants, UCI Chao Family Comprehensive Cancer Center's seed grant. T.V. is supported by NSF GRFP.

Notes and references

1. Cancer Statistics, https://www.cancer.gov/about-cancer/understanding/statistics, (accessed December 21, 2018).
2. Siegel RL, Miller KD and Jemal A, CA. Cancer J. Clin, 2018, 68, 7–30. [PubMed: 29313949]
3. NCCN Clinical Practice Guidelines in Oncology, Colon Cancer, Vers 4.2018, (accessed December 19, 2018).
4. Crowley E, Di Nicolantonio F, Loupakis F and Bardelli A, Nat. Rev. Clin. Oncol, 2013, 10, 472–484. [PubMed: 23836314]
5. Ignatiadis M and Dawson S-J, Ann. Oncol. Off. J. Eur. Soc. Med. Oncol, 2014, 25, 2304–2313.
6. Heitzer E, Haque IS, Roberts CES and Speicher MR, Nat. Rev. Genet, DOI:10.1038/s41576-018-0071-5.
7. Krebs MG, Metcalf RL, Carter L, Brady G, Blackhall FH and Dive C, Nat. Rev. Clin. Oncol, 2014, 11, 129–144. [PubMed: 24445517]
8. Alix-Panabieres C and Pantel K, Cancer Discov, 2016, 6, 479–491. [PubMed: 26969689]
9. Diehl F, Schmidt K, Choti MA, Romans K, Goodman S, Li M, Thornton K, Agrawal N, Sokoll L, Szabo SA, Kinzler KW, Vogelstein B and Diaz LAJ, Nat. Med, 2008, 14, 985–990. [PubMed: 18670422]
10. Tie J, Wang Y, Tomasetti C, Li L, Springer S, Kinde I, Silliman N, Tacey M, Wong H-L, Christie M, Kosmider S, Skinner I, Wong R, Steel M, Tran B, Desai J, Jones I, Haydon A, Hayes T, Price

TJ, Strausberg RL, Diaz LA Jr, Papadopoulos N, Kinzler KW, Vogelstein B and Gibbs P, Sci. Transl. Med, 2016, 8, 346ra92–346ra92.

11. Webb S, Nat. Biotechnol, 2016, 34, 1090. [PubMed: 27824838]
12. Schwarzenbach H, Hoon DSB and Pantel K, Nat. Rev. Cancer, 2011, 11, 426–437. [PubMed: 21562580]
13. Siravegna G, Marsoni S, Siena S and Bardelli A, Nat. Rev. Clin. Oncol, 2017, 14, 531. [PubMed: 28252003]
14. Bettegowda C, Sausen M, Leary RJ, Kinde I, Wang Y, Agrawal N, Bartlett BR, Wang H, Luber B, Alani RM, Antonarakis ES, Azad NS, Bardelli A, Brem H, Cameron JL, Lee CC, Fecher LA, Gallia GL, Gibbs P, Le D, Giuntoli RL, Goggins M, Hogarty MD, Holdhoff M, Hong S-M, Jiao Y, Juhl HH, Kim JJ, Siravegna G, Laheru DA, Lauricella C, Lim M, Lipson EJ, Marie SKN, Netto GJ, Oliner KS, Olivi A, Olsson L, Riggins GJ, Sartore-Bianchi A, Schmidt K, Shih le-M., Oba-Shinjo SM, Siena S, Theodorescu D, Tie J, Harkins TT, Veronese S, Wang T-L, Weingart JD, Wolfgang CL, Wood LD, Xing D, Hruban RH, Wu J, Allen PJ, Schmidt CM, Choti MA, Velculescu VE, Kinzler KW, Vogelstein B, Papadopoulos N and Diaz LAJ, Sci. Transl. Med, 2014, 6, 224ra24.
15. Deng R, Zhang K and Li J, Acc. Chem. Res, 2017, 50, 1059–1068. [PubMed: 28355077]
16. Deng R, Zhang K, Wang L, Ren X, Sun Y and Li J, Chem, 2018, 4, 1373–1386.
17. Tang X, Deng R, Sun Y, Ren X, Zhou M and Li J, Anal. Chem, 2018, 90, 10001–10008. [PubMed: 30016869]
18. George D, Czech J, John B, Yu M and Jennings LJ, Chimerism, 2013, 4, 102–108. [PubMed: 23974275]
19. Zhou B, Haney MS, Zhu X, Pattni R, Abyzov A and Urban AE, Methods Mol. Biol. Clifton NJ, 2018, 1768, 173–190.
20. Cao Y, Raith MR and Griffith JF, Water Res, 2015, 70, 337–349. [PubMed: 25543243]
21. Hindson BJ, Ness KD, Masquelier DA, Belgrader P, Heredia NJ, Makarewicz AJ, Bright IJ, Lucero MY, Hiddessen AL, Legler TC, Kitano TK, Hodel MR, Petersen JF, Wyatt PW, Steenblock ER, Shah PH, Bousse LJ, Troup CB, Mellen JC, Wittmann DK, Erndt NG, Cauley TH, Koehler RT, So AP, Dube S, Rose KA, Montesclaros L, Wang S, Stumbo DP, Hodges SP, Romine S, Milanovich FP, White HE, Regan JF, Karlin-Neumann GA, Hindson CM, Saxonov S and Colston BW, Anal. Chem, 2011, 83, 8604–8610. [PubMed: 22035192]
22. Ono Y, Sugitani A, Karasaki H, Ogata M, Nozaki R, Sasajima J, Yokochi T, Asahara S, Koizumi K, Ando K, Hironaka K, Daito T and Mizukami Y, Mol. Oncol, 2017, 11, 1448–1458. [PubMed: 28691390]
23. Basu AS, SLAS Technol, 2017, 22, 369–386. [PubMed: 28448765]
24. Zhang K, Kang D-K, Ali MM, Liu L, Labanieh L, Lu M, Riazifar H, Nguyen TN, Zell JA, Digman MA, Gratton E, Li J and Zhao W, Lab. Chip, 2015, 15, 4217–4226. [PubMed: 26387763]
25. Kang D-K, Ali MM, Zhang K, Huang SS, Peterson E, Digman MA, Gratton E and Zhao W, Nat. Commun, 2014, 5, 5427. [PubMed: 25391809]
26. Pekin D, Skhiri Y, Baret J-C, Le Corre D, Mazutis L, Salem CB, Millot F, El Harrak A, Hutchison JB, Larson JW, Link DR, Laurent-Puig P, Griffiths AD and Taly V, Lab. Chip, 2011, 11, 2156–2166. [PubMed: 21594292]
27. How Kit A, Mazaleyrat N, Daunay A, Nielsen HM, Terris B and Tost J, Hum. Mutat, 2013, 34, 1568–1580. [PubMed: 24038839]
28. Soh J, Okumura N, Lockwood WW, Yamamoto H, Shigematsu H, Zhang W, Chari R, Shames DS, Tang X, MacAulay C, Varella-Garcia M, Vooder T, Wistuba II, Lam S, Brekken R, Toyooka S, Minna JD, Lam WL and Gazdar AF, PloS One, 2009, 4, e7464. [PubMed: 19826477]
29. Sefrioui D, Mauger F, Leclere L, Beaussire L, Di Fiore F, Deleuze J-F, Sarafan-Vasseur N and Tost J, Clin. Chim. Acta Int. J. Clin. Chem, 2017, 465, 1–4.
30. Amstad E, Chemama M, Eggersdorfer M, Arriaga LR, Brenner MP and Weitz DA, Lab. Chip, 2016, 16, 4163–4172. [PubMed: 27714028]
31. Jeong H-H, Yelleswarapu VR, Yadavali S, Issadore D and Lee D, Lab. Chip, 2015, 15, 4387–4392. [PubMed: 26428950]

32. Diaz LAJ and Bardelli A, J. Clin. Oncol. Off. J. Am. Soc. Clin. Oncol, 2014, 32, 579–586.
33. Riva F, Dronov OI, Khomenko DI, Huguet F, Louvet C, Mariani P, Stern M-H, Lantz O, Proudhon C, Pierga J-Y and Bidard F-C, Mol. Oncol, 2016, 10, 481–493. [PubMed: 26856794]
34. Haigis KM, Trends Cancer, 2017, 3, 686–697. [PubMed: 28958387]
35. Milbury CA, Zhong Q, Lin J, Williams M, Olson J, Link DR and Hutchison B, Biomol. Detect. Quantif, 2014, 1, 8–22. [PubMed: 27920993]
36. Hatch AC, Fisher JS, Tovar AR, Hsieh AT, Lin R, Pentoney SL, Yang DL and Lee AP, Lab. Chip, 2011, 11, 3838–3845. [PubMed: 21959960]
37. Yelleswarapu VR, Jeong H-H, Yadavali S and Issadore D, Lab. Chip, 2017, 17, 1083–1094. [PubMed: 28225099]
38. Kim M, Pan M, Gai Y, Pang S, Han C, Yang C and Tang SKY, Lab. Chip, 2015, 15, 1417–1423. [PubMed: 25588522]
39. Pinheiro LB, Coleman VA, Hindson CM, Herrmann J, Hindson BJ, Bhat S and Emslie KR, Anal. Chem, 2012, 84, 1003–1011. [PubMed: 22122760]
40. Hindson CM, Chevillet JR, Briggs HA, Gallichotte EN, Ruf IK, Hindson BJ, Vessella RL and Tewari M, Nat. Methods, 2013, 10, 1003–1005. [PubMed: 23995387]
41. Kang Q, Parkin B, Giraldez MD and Tewari M, BioTechniques, 2016, 60, 175–176, 178, 180 passim. [PubMed: 27071606]
42. Whale AS, Devonshire AS, Karlin-Neumann G, Regan J, Javier L, Cowen S, Fernandez-Gonzalez A, Jones GM, Redshaw N, Beck J, Berger AW, Combaret V, Dahl Kjersgaard N, Davis L, Fina F, Forshew T, Fredslund Andersen R, Galbiati S, González Hernández Á, Haynes CA, Janku F, Lacave R, Lee J, Mistry V, Pender A, Pradines A, Proudhon C, Saal LH, Stieglitz E, Ulrich B, Foy CA, Parkes H, Tzonev S and Huggett JF, Anal. Chem, 2017, 89, 1724–1733. [PubMed: 27935690]
43. Dong L, Wang S, Fu B and Wang J, Sci. Rep, 2018, 8, 9650–9650. [PubMed: 30504843]
44. Demuth C, Spindler K-LG, Johansen JS, Pallisgaard N, Nielsen D, Hogdall E, Vittrup B and Sorensen BS, Transl. Oncol, 2018, 11, 1220–1224. [PubMed: 30086420]
45. Denis JA, Patroni A, Guillerm E, Pepin D, Benali-Furet N, Wechsler J, Manceau G, Bernard M, Coulet F, Larsen AK, Karoui M and Lacorte J-M, Mol. Oncol, 2016, 10, 1221–1231. [PubMed: 27311775]
46. Millner LM, Linder MW and Valdes R Jr, Ann. Clin. Lab. Sci, 2013, 43, 295–304. [PubMed: 23884225]
47. Gabriel MT, Calleja LR, Chalopin A, Ory B and Heymann D, Clin. Chem, 2016, 62, 571–581. [PubMed: 26896446]

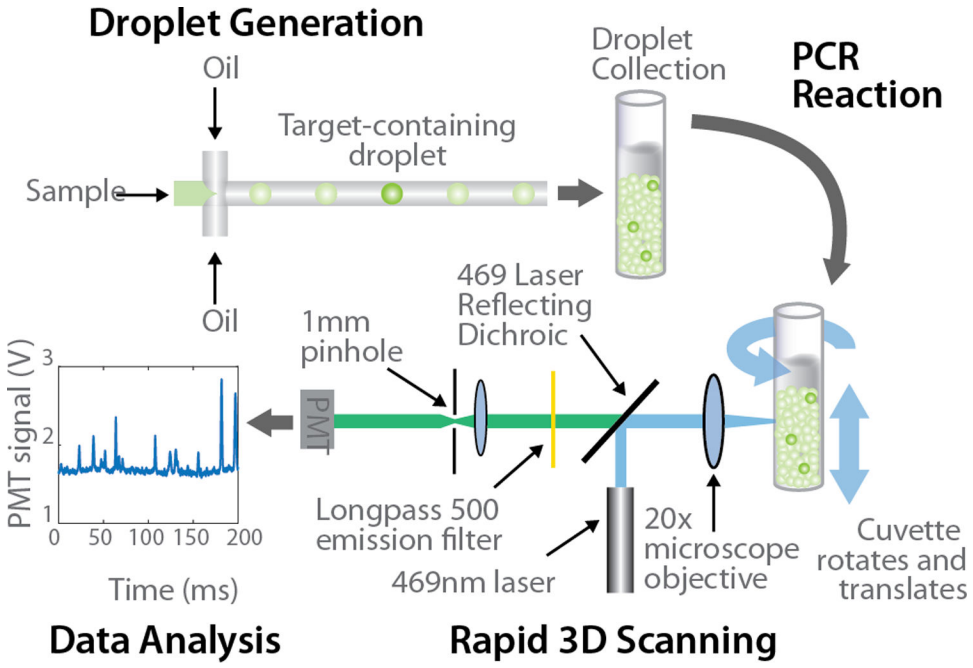

Figure 1.

IC3D ddPCR workflow diagram for a typical clinical sample. The IC3D technology involves partitioning a sample into millions of picoliter-sized droplets, thermocycling the droplets to amplify specific fluorescent signals, and detecting/quantifying droplets that are positive for one or more specific targets. Unlike commercial dPCR systems, the IC3D technology can analyze large sample volumes with great number of partitions, which can collectively improve sensitivity of ctDNA detection.

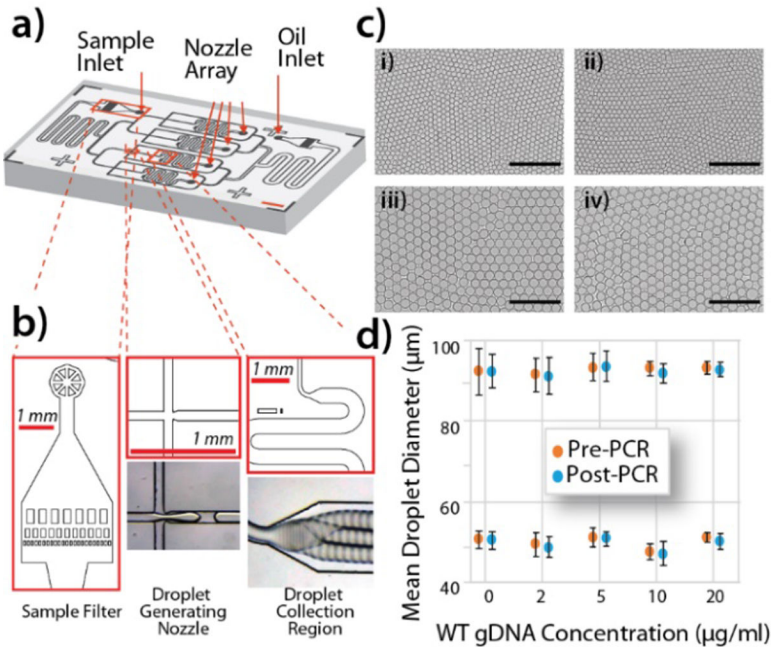

Figure 2. High-throughput droplet generation and thermocycling stability.

A) Schematic of custom droplet generation chip with inlets and outlets identified. B) Close-up view of three important features including: integrated sample and oil filter, droplet generating nozzle array (flow-focusing principle), and droplet collection region. C) Brightfield microscope images of a 2D monolayer of droplets in a hemocytometer, i) 50 μm droplets pre-PCR, ii) 50 μm droplets post-PCR, iii) 90 μm droplets pre-PCR, iv) 90 μm droplets post-PCR. Scale bar = 500 μm. D) Quantitative measurements of individual droplet diameters demonstrate robust droplet stability before and after thermocycling across a range of gDNA concentrations from 0–20 μg/ml.

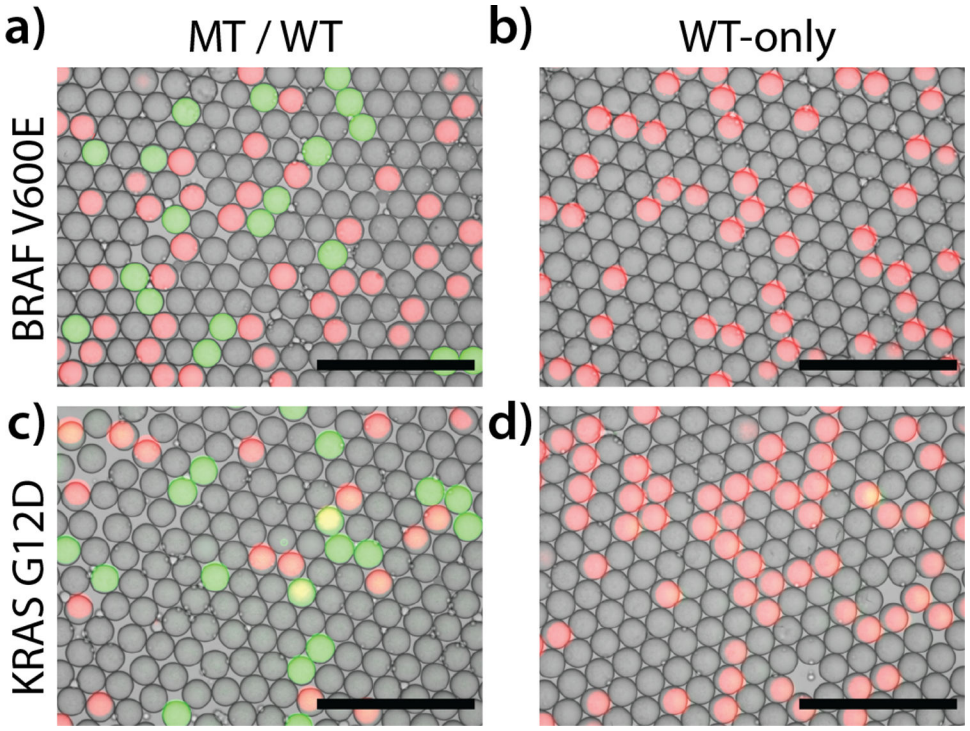

Figure 3.

Fluorescent microscope images of droplets with different target mutations. RGB multichannel images composed of brightfield droplet image (grey), MT-specific probe (FAM fluorophore) (green), and WT-specific probe (CAL560 fluorophore) (red). Scale bar = 500 μm.

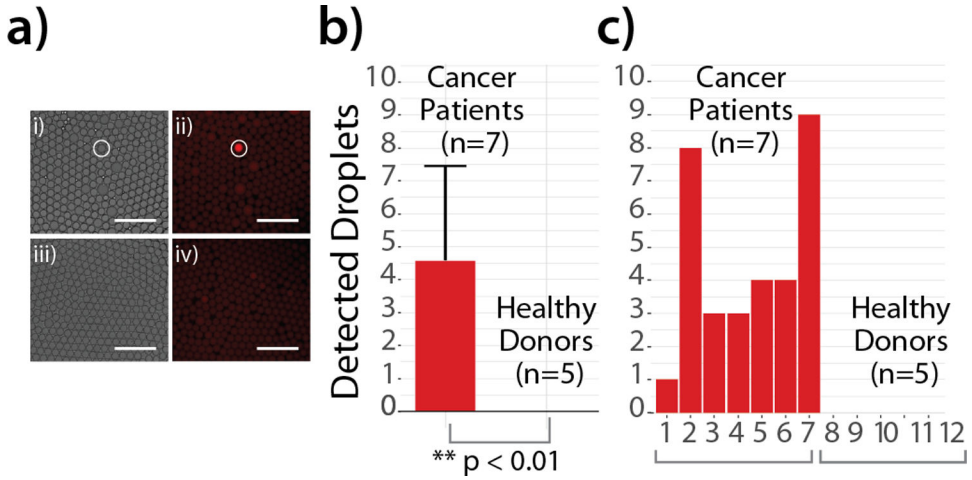

Figure 4.

Analysis of KRAS G12+ CRC patient plasma samples using our droplet PCR assay. a) Representative fluorescent microscope images of droplets following PCR from a Stage IIA cancer patient (i – BF, ii – fluorescent) and a control healthy patient (iii – BF, iv – fluorescent) (Scale bar = 500 μm). Positive droplets were defined as those with a signal-to-noise ratio (SNR) greater than 3.0 and then enumerated in group (b) or as individual patient (c). Y axis = number of detected droplets in 100 μl final volume.

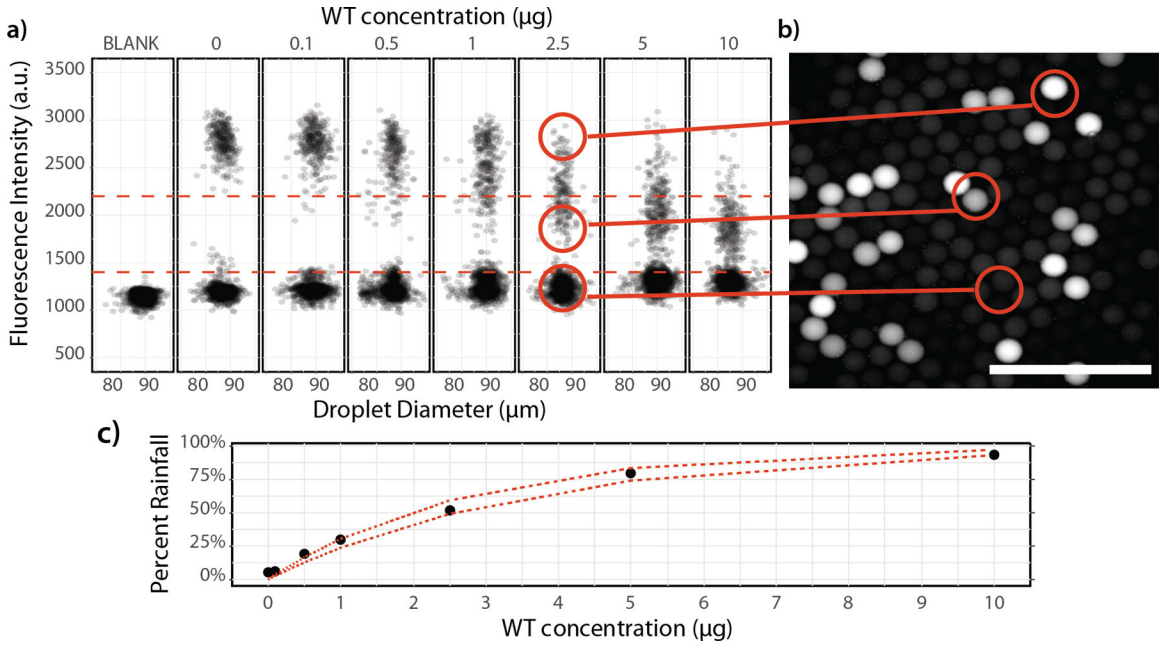

Figure 5.

Effect of number of partitions on assay performance. A) Calculated percent rainfall (intermediate droplet fraction / total positive droplet fraction) from droplet intensity data in Panel B.B. Dashed red lines refer to the lower and upper boundaries of the “intermediate-intensity” zone, where droplets are distinguished from empty (“negative”) droplets and fully amplified droplets. B) Raw fluorescence intensity data collected for partitioning experiment. C) Agreement with paritioning theory. Solid circles represent calculated percent rainfall from panel A. Dotted red lines refers to upper and lower 95% confidence interval for theoretical percent rainfall given MT and WT copy numbers and an average droplet diameter of 90µm.

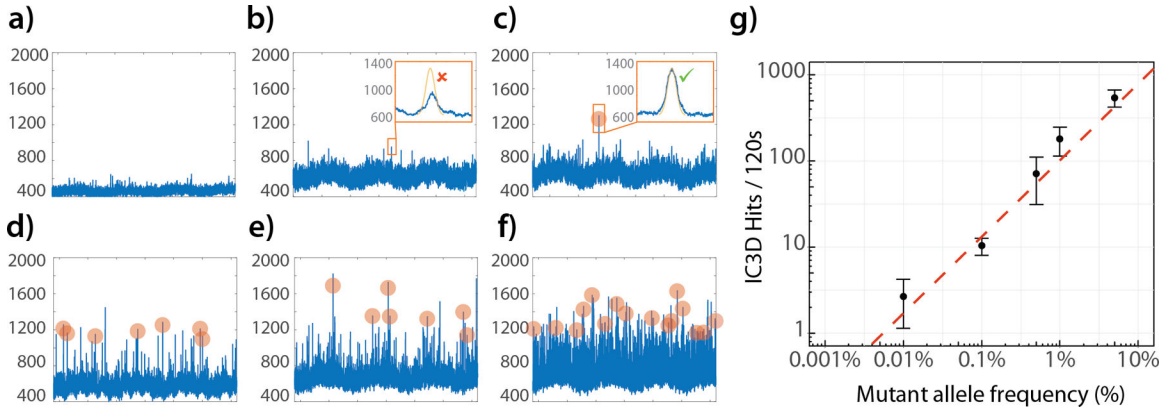

Figure 6.

Detection of synthetic KRAS G12D mutant in Jurkat gDNA by IC3D. Panels A-F: raw fluorescent time trace data (y-axis = PMT signal (mV), x-axis = 5 seconds acquisition time): a) Blank, b) 0 % AF, c) 0.1% AF, d) 0.5% AF, e) 1% AF, f) 5% AF. Orange circles denote confirmed positive droplet. G) Concentration curvve of detected positive droplets versus %AF. Points represent combined average of three replicates. (Error bars denote ± standard deviation, n=3).

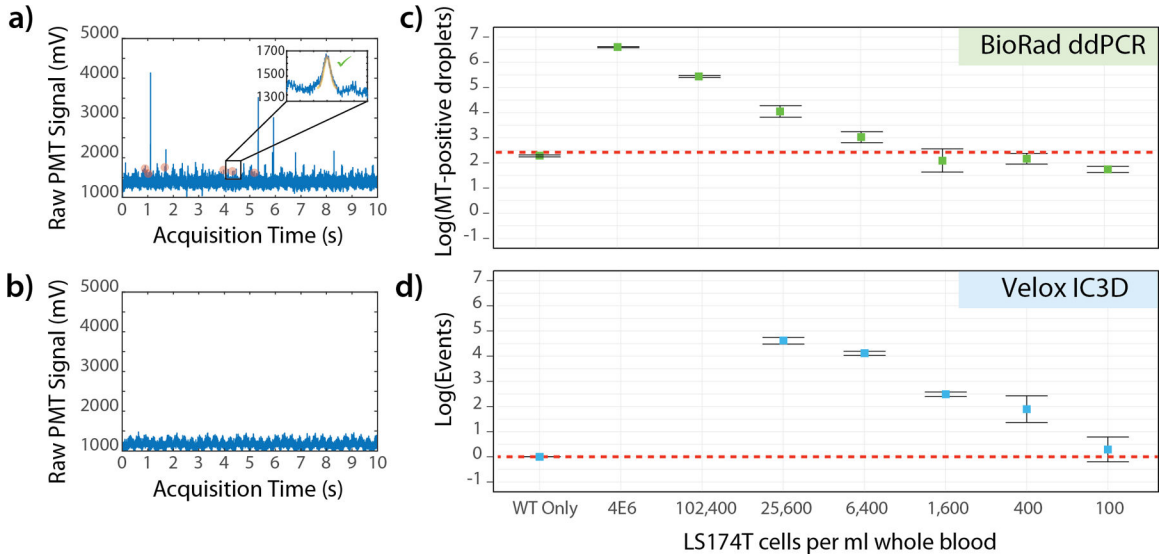

Figure 7.

Detection of spiked LS174T in whole blood using IC3D. Panels A and B represent raw fluorescent time trace data recorded on IC3D for a positive sample (1,600 cells/ml) and negative sample, respectively. The inset in Panel A is of a representative positive event where the shape-fitting algorithm criteria was met and displayed over an x-axis of 6 ms. Panels C and D demonstrate the sensitivity of the Bio-Rad ddPCR and IC3D systems for the detection of KRAS G12D mutations as a genetic approach for quantifying CTCs in whole blood extractions. C) Bio-Rad ddPCR results; y-axis = log reported Poisson MT-positive droplets, red dashed line = false positive rate based on events detected in WT-only negative control, error bars = relative error bar (for symmetrical display on log-scale), defined as ±0.434*stDev/y across 2 replicate wells. D) IC3D results; y-axis = = log events (per 120s), error bars = relative error (described above) across 3 independent sample replicates.